sciendo

CIVIL AND ENVIRONMENTAL ENGINEERING REPORTS

E-ISSN 2450-8594

CEER 2020; 30 (3): 0214-0233
DOI: 10.2478/ceer-2020-0041
Original Research Article

STABILITY OF ANCHORED RETAINING WALLS UNDER SEISMIC LOADING CONDITIONS TO OBTAIN MINIMAL ANCHOR LENGTHS USING THE IMPROVED FAILURE MODEL

Fatima Zohra BENAMARA[1], Ammar ROUAIGUIA[2], Messaouda BENCHEIKH[3]
[123] Civil Engineering and Hydraulic Department, 8 Mai 1945 University, Guelma, Algeria
[13]Laboratory of Civil Engineering and Hydraulics, 8 Mai 1945 University, Guelma, Algeria

Abstract

Anchored retaining walls are structures designed to support different loading applied in static and dynamic cases. The purpose of this work is to design and study the stability of an anchored retaining wall loaded with different seismic actions to obtain minimal anchor lengths. Mononobe-Okabe theory has been applied for the evaluation of seismic earth pressures developed behind the anchored wall. Checking the dynamic stability of anchored retaining walls is usually done using the classic Kranz model. To take into consideration the effects of the internal forces developed during failure, we have proposed a new model, based on the Kranz model, which will be used as the Kranz model to find the critical angle failure performed iteratively until the required horizontal

[1] Corresponding author: Civil Engineering and Hydraulic Department, 8 mai 1945 Guelma University, Box.401.Guelma. Algeria, e-mail: benamara_fati2003@yahoo.fr or benamara.fatimazohra@univ-guelma.dz

anchor length is reached for a minimum safety factor. The results of this study confirm that the effect of the seismic load on the design of an anchored retaining wall, and its stability, has a considerable influence on the estimation of anchor lengths. To validate the modifications made to the new model, a numerical analysis was carried out using the Plaxis 2D software. The interpretation of the obtained results may provide more detailed explanation on the effect of seismic intensities for the design of anchored retaining walls.

Keywords: anchored walls, safety factor, pseudo static, seismic earth pressure, failure model, Plaxis2D

1. INTRODUCTION

Anchored retaining walls are used to stabilize excavations and slopes. Stability analysis of anchored retaining walls under static and dynamic loading is an important step in the design of such structures [6]. Estimation of the seismic earth pressure is also important for the safe design of anchored retaining walls in a seismic zone. Mononobe-Okabe theory [9] is the most widely used method to determine the lateral seismic earth pressure of cohesionless soils and rigid retaining walls [12]. Using the pseudo-static approach, several researchers have developed different methods to determine the seismic earth pressure considering $c-\varphi$ backfill soil on a rigid retaining wall, without considering the roughness of the wall, and also without taking into account the effect of tension cracking while adopting the planar single-wedge method in the seismic analysis [13].

In the current study, an analytical procedure predicting the seismic earth pressures in c-φ soils is proposed for the seismic design and stability of anchored retaining walls [14]. The effect of tension cracking was considered and the roughness of the retaining anchored wall was also taken into consideration [7]. In addition, the rigid double-wedge failure mechanism was used to analyze the stability of the anchored retaining walls [8].

The design of the anchored retaining wall and its stability checks were carried out under different seismic loadings by varying the seismic coefficient k_h using Kranz's failure model [11].

In this study, a new model has been proposed, based on Kranz models [5] but with some modifications such as varying the inclination of the secondary slip surface (ρ) and considering the effect of the cohesive force (C_2) on this slip [2].

To validate these changes, a series of finite element calculations were performed using Plaxis 8.6 software [3]. The results were presented and compared with the results of the analytical approach.

2. DESIGN OF ANCHORED RETAINING WALL

As stated above, an analytical procedure with a pseudo-static method for predicting the seismic earth pressures in c-φ soils is proposed for the seismic design of the anchored retaining wall. The free earth support method was adopted for deducing the wall embedment depth (f), the anchor force (T), and the maximum moment as presented in Table 1. The geometry, soil conditions, and surcharge adopted in the present analysis are given in Fig. 1.

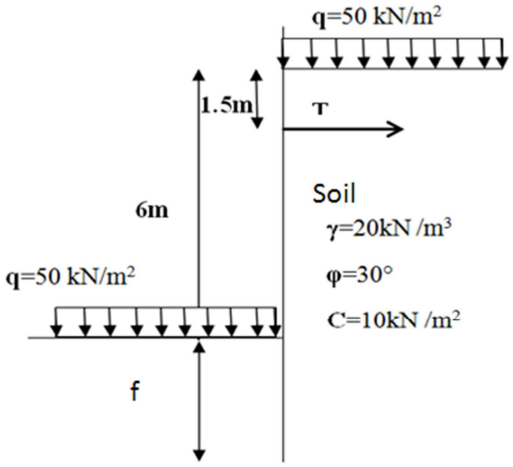

Fig. 1. Standard anchored wall profile

According to RPA [1], k_h and k_v are the seismic acceleration coefficients in the horizontal and vertical directions, respectively. They should be taken into account and can be expressed as follows: $K_h = A * a$ and $k_V = \pm 0.3\, k_h$, where (A) is the zone acceleration coefficient and $a = (\%\, g)$ is the acceleration in the g unit. Tables 1 and 2 present a detailed calculation of different seismic accelerations k_h = (0.05, 0.10, 0.15, and 0.20) (g). The roughness of the anchored retaining wall is the friction angle between the wall and the soil, and has been taken as ($\delta_a = ((2/3)\, \varphi)$ for the evaluation of active earth pressure [4,10].

Table 1. Calculation results of the anchor force (T), the wall embedment depth (f), and the moment M (z) for the case (k_h; + k_v)

k_h	0.05	0.10	0.15	0.20
k_v	0.015	0.03	0.045	0.06
f (m)	2.35	2.95	3.80	5.20
T(kN)	115.8	130.41	153.07	184.85
M(z) (kN.m)	134.12	168.36	217.83	275.23

Table 2. Calculation results of the anchor force (T), the wall embedment depth (f), and the moment M (z) for the case (k_h; - k_v)

k_h	0,05	0,10	0,15	0,20
k_V	- 0.015	- 0.03	- 0.045	- 0.06
f (m)	2.34	2.85	3.55	4.5
T(kN)	117.81	134.53	160.79	190.09
M(z) (kN.m)	140.64	171.95	212.51	269.61

3. DYNAMIC STABILITY STUDY WITH FAILURE MODELS

3.1. Kranz model

The Kranz model was used to check the stability of the anchored retaining wall. The failure mechanism is defined by the principal failure line that cuts the bond length (L_0) at the center and divides it into two secondary sliding surfaces. This model is characterized by a rigid wedge (1) in which the following forces are applied: the reaction of the anchor (T), the reaction of the wall on that wedge (p_{ah}^{E}), the friction of the soil on the main failure line (R), the cohesion force (C), the overload (P) and the weight of the wedge (1) (G). The seismic active earth pressure (p_{ah1}^{E}) replaces the wedge action (2) on the wedge (1) through the secondary slip surface considered as a fictitious vertical wall. The inter-wedge friction angle ($\delta_f=\varphi$) is used (Fig. 2).

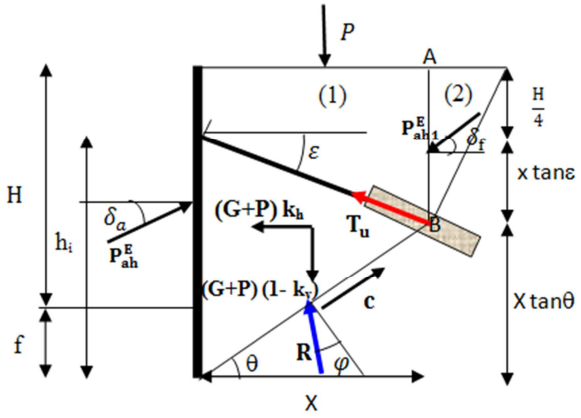

Fig. 2. The applied forces on the rigid body in the Kranz model under dynamic loading.

The safety factor defined by Kranz was given by (Eq.3.1).

$$F_s = \frac{T_u}{T} \tag{3.1}$$

Where, T_u= the ultimate pullout capacity of the anchor

T= the mobilized capacity of the anchor

The forces applied to the models are calculated according to the anchor length (X) given by (Eq. 3.2).

$$X = \frac{(3H/4) + f}{(\tan(\varepsilon)+\tan(\theta))} \tag{3.2}$$

The equilibrium study of vertical and horizontal forces gives us, after algebraic transformation (Eq. 3.3).

$$T_{uh} = \frac{\left[(G+P)(1-k_v + k_h)\text{-}P_{ah}^E \tan(\delta_a) - C\sin\theta\right]\tan(\theta\text{-}\varphi)\text{-}P_{ah}^E + P_{ah1}^E - C\cos\theta}{\tan(\varepsilon) + \tan(\theta - \varphi) - 1} \tag{3.3}$$

The failure angle (θ) is varying iteratively to find the horizontal anchor length (X) corresponding to a minimum safety factor (F_s) given by (Eq. 3.1). The forces described by (Eq. 3.3) are calculated according to the anchor length (X) given by (Eq.3.2).The anchor lengths are determined for the different values of k_h. The comparative results of studies for different failure angles are presented in Table 3.

Table 3. The results of the anchor length calculations for different horizontal seismic coefficients k_h

k_h	T (kN)	f(m)	θ (°)	G(kN)	P(kN)	p_{ah}^{E} (kN)	p_{ah1}^{E} (kN)	C(kN)	L(m)
0.05	115.8	2.35	11.70	338.25	246.90	271.00	41.23	49.38	5.11
0.10	130.4	2.95	13.60	430.85	289.16	338.34	51.9	57.83	5.98
0.15	153.0	3.80	15.32	581.9	350.56	442.14	68.82	70.11	7.25
0.20	184.8	5.20	17.42	856.95	446.88	631.00	98..42	89.57	9.25

3.2. Improved Kranz Model

Based on the Kranz model, a new model has been proposed, characterized by a secondary sliding surface inclined at an angle (ρ) with the vertical as shown in Fig. 3. The proposed model considers the friction between the two rigid solids $\delta_f=\varphi$ and the cohesion force C_2 applied on the secondary slip surface.

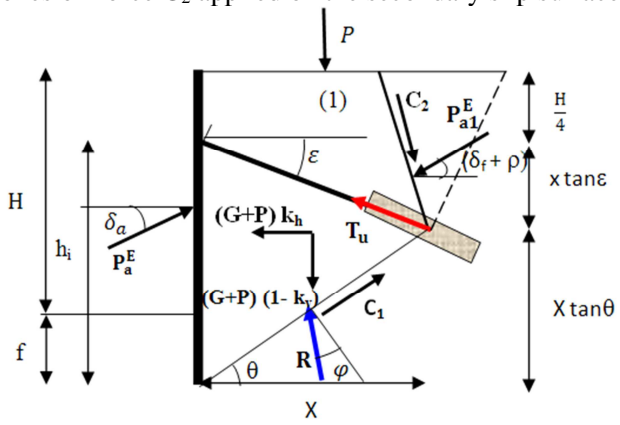

Fig. 3. The applied forces on the rigid body in the Improved Kranz model under dynamic loading

Equation (3.4) is obtained after algebraic transformation of the equilibrium of vertical and horizontal forces, as shown below.

$$\left[(G+P)(1 - k_v + k_h) + P_{a1h}\tan(\delta_f + \rho) + C_{2v})\tan(\theta-\varphi) + 1.5\ T_{uh} + P_{a1h}\right] - \left[(P_{ah}\tan(\delta_a) + 1.5\ T_{uh}\tan(\varepsilon) + C_{1h}\tan(\theta)\tan(\theta-\varphi) + P_{ah} + C_{1h} + C_{2v}\tan(\rho)\right] = 0 \quad (3.4)$$

Where C_{2v} and C_{1h} are the vertical components of the cohesion force C_2 and the horizontal component of the cohesion force C_1, respectively; P_{ah} is the horizontal component of the earth pressure P_a; and P_{a1h} is the horizontal component of the earth pressure P_{a1}.

In this study, the angle (ρ) varies between +5 and -5 in order to achieve the minimum anchor lengths for a safety factor equal to 1.5. The main results are presented in Tables 4 and 5.

Table 4. Results of the calculations of the anchor lengths for ρ = +5[°]

k_h	T(kN)	f(m)	θ(°)	G(kN)	p^E_{ah} (kN)	p^E_{ah1} (kN)	C_{1h}(kN)	C_{2v}(kN)	L(m)
0.05	115.8	2.35	12.42	326.31	271.0	45.67	48.12	28.00	4.98
0.10	130.4	2.95	14.20	419.38	338.34	57.21	56.62	30.28	5.86
0.15	153.0	3.80	15.82	571.35	442.13	75.58	68.91	33.59	7.13
0.20	184.8	5.20	17.81	859..68	631.00	108.11	88.24	38.79	9.13

Table 5. Results of the calculations of the anchor lengths for ρ = -5[°]

k_h	T(kN)	f(m)	θ(°)	G(kN)	p^E_{ah} (kN)	p^E_{ah1} (kN)	C_{1h}(kN)	C_{2v}(kN)	L(m)
0.05	115.8	2.35	13.17	424.1	271.00	34.96	46.80	27.64	4.84
0.10	130.4	2.95	14.90	413.92	338.34	44.43	59.20	29.90	5.71
0.15	153.0	3.80	16.50	559.95	442.13	59.30	67.35	33.17	6.97
0.20	184.8	5.20	18.45	835.59	631.00	85.57	86.42	38.30	8.94

3.3. Comparison of Failure Models

For different seismic horizontal coefficients and different active earth pressures behind the secondary failure surface, the anchor lengths for Kranz and Improved Kranz models were computed. As shown in Fig. 4, the Kranz model suggested higher anchor lengths (from 5.11 m to 9.25 m) compared to the Improved Kranz model for different variations of (k_h). The suggested model provided shorter

lengths (from 4.84 m to 8.94 m) applied for different horizontal seismic coefficients.

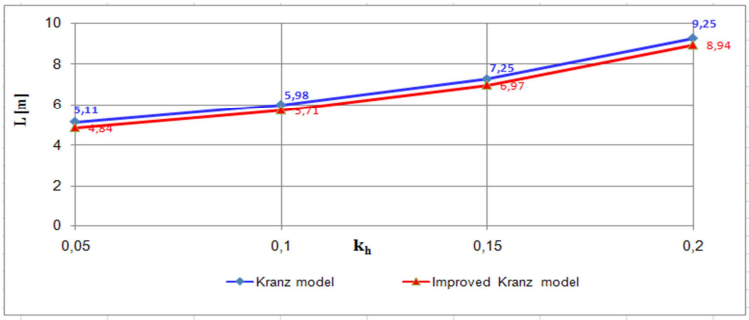

Fig. 4. Comparison of anchor lengths between Kranz and Improved Kranz models

It can be noted that for the (k_h) = (0.20) using the improved Kranz model, the anchor length reduces from 9.25 m for ρ =0 to 8.94 m for ρ =-5°. Similarly, the earth pressure P_{a1h} reduces from 98.42 to 85.57 kN/m for the same values of ρ. As shown in Fig. 5, the cohesion force (C_2) applied on the secondary failure surface is higher the more powerful the earthquake is, the same is evident for the seismic active earth pressures developed behind the fictitious wall.

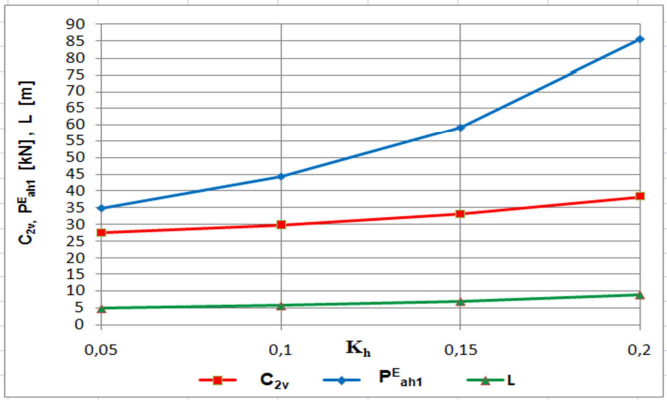

Fig 5. The effect of active earth pressures p^E_{ah1} and cohesion force (C_{2v}) on the anchor lengths

From Figs. 6 and 7, it can be noted that the earth pressure (P_{ah1}) acting on the secondary sliding surface was decreased in the improved model for the same horizontal seismic coefficient. The anchor lengths were even shorter when the earth pressure decreased behind a secondary failure surface that is inclined by an angle of ρ=-5° and a cohesion force (C_2) is applied on the same sliding surface.

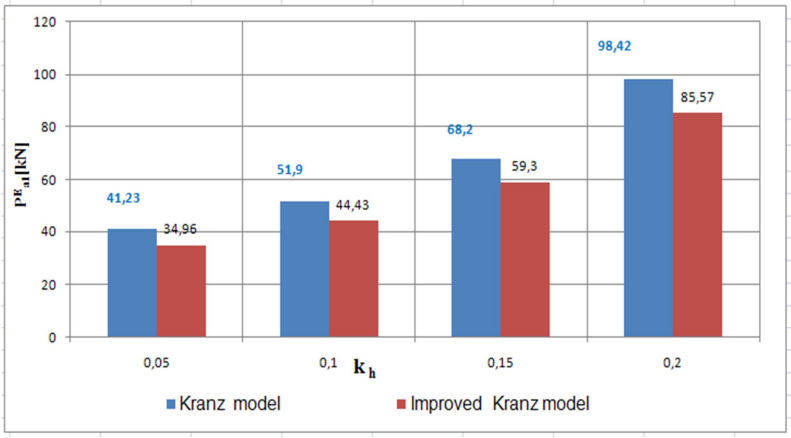

Fig. 6. The effect of the earth pressure p^{E}_{ah1} on anchor lengths

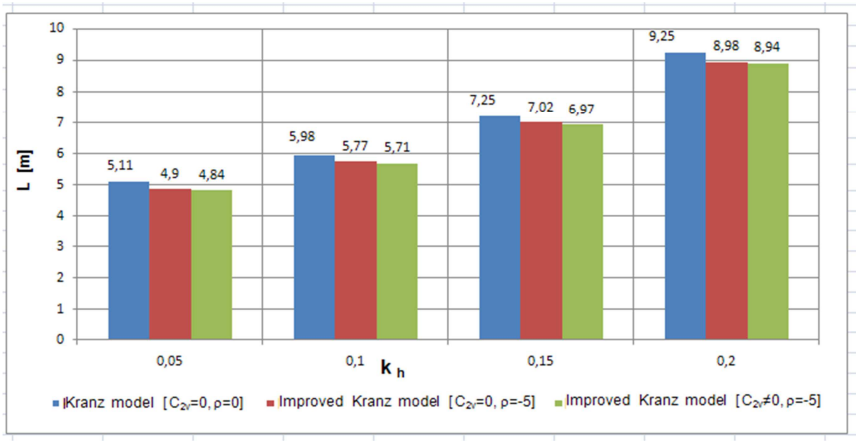

Fig. 7. The effect of the acting cohesion force C_{2v} to the secondary sliding surface on anchors lengths

3.4 Results

Determination of the wall embedment depth and the maximum moment determined by using the seismic coefficient ($+k_v$) were found to be higher than those determined with ($-k_v$), as a result, the component of the downward seismic acceleration is less favorable than the ascending component. The wall embedment depth and the moment both increase with the increase in the seismic coefficient (k_h).

With respect to the Kranz model, the anchor force (T_{uh}) increases with the increase of the seismic coefficient. Similarly, the anchor lengths increase with the increase of the seismic load. This is due to the increase of the failure angle (θ).

The equations of the proposed model are improved by taking into account the effects of internal forces such as cohesion, friction between wedges as well as the inclined sliding surface. The consideration of the internal force (C_2) and the inclination of the slip surface can provide high accuracy in the calculation of anchor lengths

4. DYNAMIC STABILITY STUDY WITH PLAXIS 2D SOFTWARE

In this work, the finite element method has been performed using the Plaxis 2D program. The FE model size of the anchored retaining wall was 30m wide and 14m high. The boundaries of the model are fixed laterally on both sides, and horizontally and vertically at the bottom boundary, as shown in fig. 8. The profile used a simple linear elastic perfectly plastic Mohr Coulomb model. Alongside the wall, the element “interface” has been used with a double aim. The interface pretends to eliminate the stress and deformation peaks produced at the corner of a structure. At the same time, the soil structure interaction is simulated by decreasing the soil resistance in this contact. The effect of the dynamic soil-structure interaction is taken into account by employing the strength reduction factor R_{rigid}=1. Interfaces on both sides of the wall are used to reproduce the effects of interaction between the soil and the wall.

Numerical analyses were performed under drained conditions using geometric and geotechnical parameters for the analytical procedure of standard profile, as described in Table 6.

Table 6. Soil parameters

Mohr-Coulomb		Material: soil Drained
γ_{sat}	[kN/m³]	20
K_x	[m/jour]	0
K_y	[m/jour]	0
E_{ref}	[kN/m²]	3000
ν		0.3
φ	[°]	30
C	[kN/m²]	10
ψ	[°]	0
R_{inter}		1
α		2.088
β		0.00156

In this study, we considered an anchor head of 1.5 m depth, inclined at 15°. The free anchor length is 4 m and the bond length is 3 m. From the analytical study, we have dimensioned the anchored retaining wall determining the wall embedment depth, the anchoring effort, and the maximum moment, thus allowing to choose the appropriate profile of walls, which is sheet pile Ian (Fig. 8).

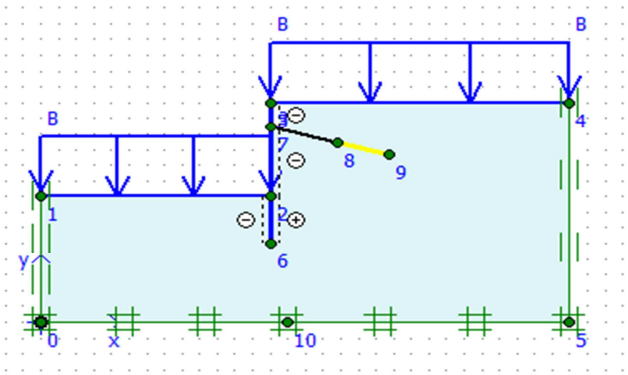

Fig. 8. Modeling the retaining wall profile

The wall was modeled using plate elements. In Plaxis, beams are modeled by plates which represent structural elements. The characteristics of the anchored

wall are defined in Table 7. Alongside the wall, the element interface was used with a double aim.

Table 7. Anchor retaining wall characteristics

Parameter	Value	Unit
Type of behavior	elastic	
normal rigidity (EA)	2373000	kN/m
Flexural rigidity (EI)	13944	kNm²/m
Poisson coefficient	0.3	

The anchor level is modeled by a combination of a node-to-node anchor (free length) and a concrete beam (bond length). The material of the node-to-node anchor is assumed to be linear-elastic and allows the transmission of load from one to another element. The geogrid was fixed at the end of the node-to-node anchor. It can represent a linear element in order to distribute the loads transferred by the free length as shown in Fig. 8. The characteristics of the anchor are shown in Table 8.

Fig. 10 shows the initial mesh of anchored retaining wall of the numerical model. Two-dimensional plane strain triangular mesh elements with 6 displacement nodes are used for the soil body as shown in figure 9. The generation of the mesh is carried out with a fine distribution element. The mesh contains 560 elements and 4685 nodes, as shown in Fig. 10.

Table 8. Anchor characteristics

Parameter	Value	Unit
Type of behavior	Elastic	
normal rigidity (EA)	750000	kN/m
Spacing (L_s)	1	M

Fig. 9. Triangular element with 6 node points

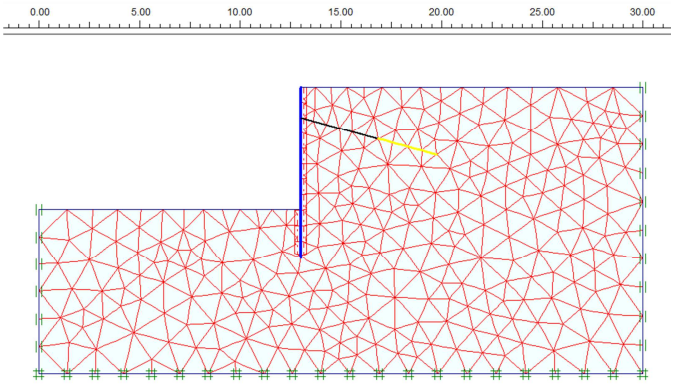

Fig. 10. Initial mesh of anchored retaining wall

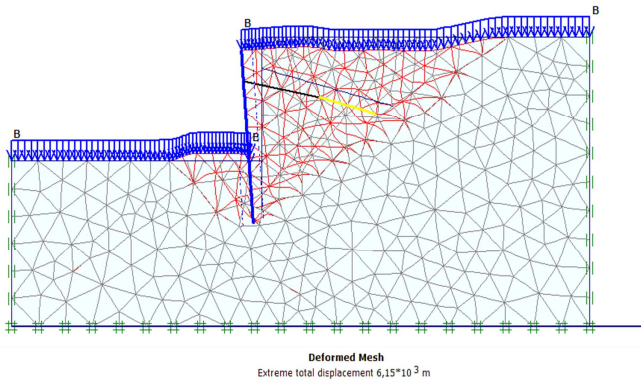

Fig. 11. Deformed mesh of anchored retaining wall

From the stability analysis of the profile anchored retaining wall, made with Plaxis 8.6 software, we can deduce the anchor force in the free length of the anchor (T_L) and the axial force (T_s) in the bond length of anchor, as shown in (Fig. 12). The maximum bending moments as well as the safety factors are determined for the case ($+k_v$) as shown in table 9.

Table 9. The anchor force (T), the maximum bending moment, and the safety factors for the case (k_h; k_v)

k_h	0.05	0.10	0.15	0.20
k_v	0.015	0.03	0.045	0.06
f (m)	2.35	2.95	3.80	5.20
T_L(kN)	157.80	204.30	223.80	225.80
T_S(kN)	134.06	182.83	199.45	200.66
M(z) (kN.m)	311.86	344.64	311.90	277.39
F_s	1.685	1.650	1.597	1.580

The maximum bending moments, the anchor forces, and the safety factors are also determined for the case ($- k_v$) as shown in table 10.

Table 10. The anchor force (T), the maximum bending moment, and the safety factors for the case (k_h;$- k_v$)

k_h	0.05	0.10	0.15	0.20
$-k_v$	-0.015	-0.03	-0.045	-0.06
f (m)	2.35	2.95	3.80	5.20
T_L(kN)	154.66	196.400	211.200	206.20
T_S(kN)	131.89	176.78	190.57	183.67
M(z) (kN.m)	301.12	325.29	285.66	262.31
F_S	1.666	1.662	1.601	1.566

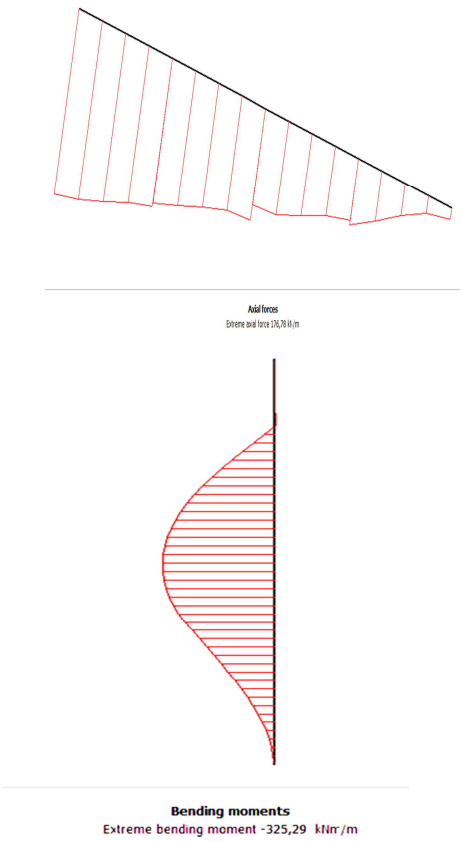

Fig. 12. Axial force in bond length of anchor and maximum bending moment in wall for k_h=0.1and k_v=-0.03

As shown in Figures 13 and 14, it can be seen that the horizontal and vertical displacements obtained from Plaxis 8.6, confirm the improved Kranz model.

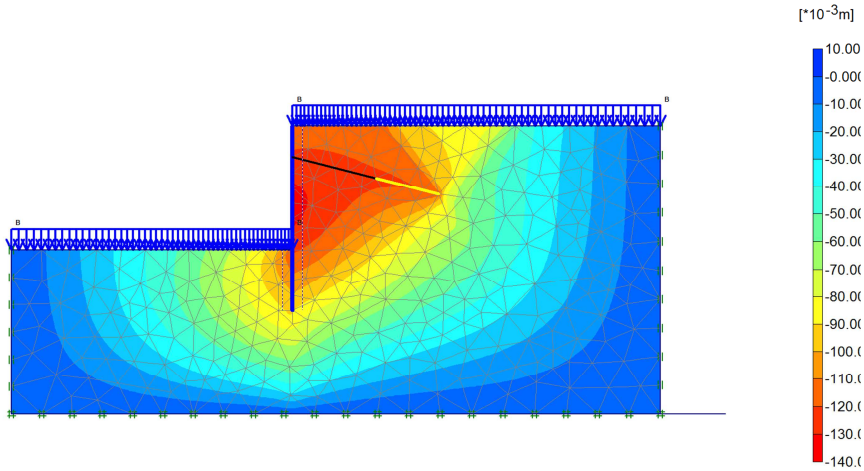

Fig. 13. Horizontal displacements for k_h=0.1 and k_v=-0.03

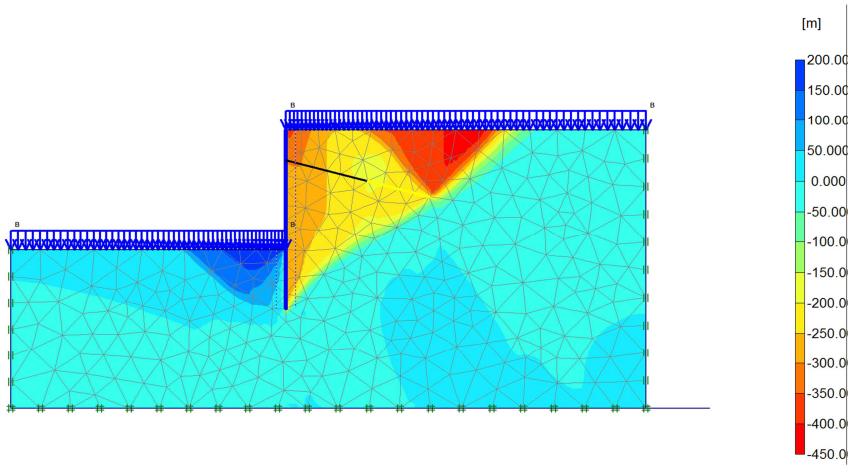

Fig. 14. Vertical displacements for k_h=0.1 and k_v=-0.03

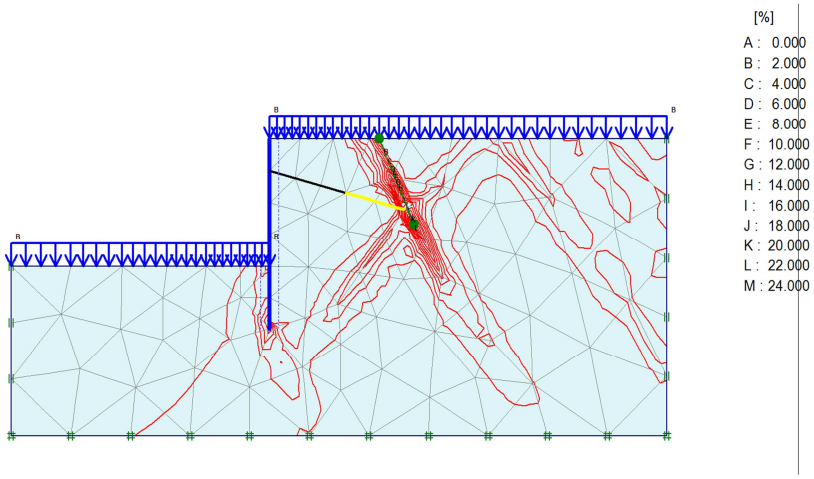

Fig. 15. Shear strains for k_h=0.1 and k_v=-0.03

4.1 Discussion of results

The numerical study carried out using the PLAXIS 8.6 software, enabled the determination of the anchoring forces in the free lengths, the axial forces in the bond lengths, and the maximum bending moments in the wall, for different horizontal and vertical seismic coefficients (k_h;; k_v).

The anchor forces and the bending moments obtained from the numerical study are greater than those determined analytically.

From tables 9 and 10, it can be concluded that the seismic acceleration coefficients (-k_v) provide maximum bending moments and greater anchor forces than those determined with (k_v) and, regarding stability, we can conclude that the anchored retaining walls verified with (-k_v) are more stable than those with (k_v).

The safety factors decrease with the increase of the horizontal seismic acceleration coefficient k_h whatever the sign of k_v. The same observation can be reported for the maximum bending moments. On the other hand, we notice an increase in anchor forces.

According to figures 13 and 14, we can distinguish the formation of two rigid solids behind the wall, separated by an inclined secondary sliding line and not vertical, which confirms the improvement made to the Kranz model.

The presence of a cohesive force on the failure line causes sliding in translation between the wedges, as a result, the failure line will be at an inclined plane as shown in Figures 13, 14, and 15. This analysis demonstrates horizontal and

vertical displacements which suggest a failure mechanism similar to the improved model.

5. CONCLUSION

The purpose of this study was to design an anchored retaining wall and to verify its stability under seismic loading. An improved model based on a classical Kranz model was proposed to verify the stability of an anchored retaining wall and to determine the anchor lengths for each horizontal seismic coefficient (k_h). The mononobe-okabe method is applied for the estimation of the seismic earth pressures for the design of the anchored retaining wall. The stability study of the anchored retaining wall with an improved Kranz model has shown that the variation of inclination of the secondary slip surface (ρ), and considering the effect of the cohesive force C_2 on this slip surface, gives shorter anchor lengths than those determined from the classical Kranz model.

A numerical study was carried out on the standard profile of the anchored retaining wall analyzed using the Plaxis 8.6 software in order to check the stability of the anchored retaining wall, and to validate the modifications made to the improved Kranz model. It is worth noting that the results of the stability analysis, such as the anchor forces and the maximum bending moments, are more or less significant compared to the analytical study. The failure mechanism obtained from plaxis analysis confirms the modifications made to the classical Kranz model by varying the inclination of the secondary sliding surface. However, the proposed model remains applicable for moderately rubbing soils which do not present dilatancy.

ADDITIONAL INFORMATION

L_0 The bond length;

c Cohesion;

θ The critical inclination of a deep-slip surface;

ε Inclination of anchor with the horizontal;

φ Friction angle of soil;

p_{ah}^{E} The horizontal component of the dynamic active earth pressure applied on the retaining wall;

p_{ah1}^{E} The horizontal component of dynamic active earth pressure on the vertical secondary slip surface;

C_{1h} The horizontal component of cohesion force on the principal failure surface;
δ_f The active angle wall friction;
β Backfill angle;
γ Soil unit weight;
f The wall embedment depth.

REFERENCES

1. Algerian Paraseismic codes RPA 99/2003 version <Règles Parasismiques Algériennes RPA99/version2003> 2003. National Center for Applied Research in Earthquake Engineering. Centre National de recherche appliquée en Génie parasismique, Algéria.
2. Benamara, FZ, Belabed, L and Rouaiguia, A 2019. Proposed Improvements To Analytical Models of Anchored Retaining Walls. *Environmental and Engineering Geoscience* **25,** 115–126.
3. Brinkgreve, RBJ 2003. Manuel de référence de PLAXIS Version 8.6. Delft University of Technology and PLAXIS bv. Pays-Bas.
4. Choudhury, D and Ahmad, SM 2007. Stability of waterfront retaining wall subjected to pseudo-static earthquake forces. *Ocean Engineering* **34**, 1947-1954.
5. Corfdi, A 2008. Kranz's method from yesterday to day: a critical review. *Revue française de géotechnique* **12**, 19–30.
6. Costet, J and Sanglerat, G 1988. *Practical course in soil mechanics 2 Calculation of structures. Cours pratique de mécanique des Sol 2 calcul des ouvrages*. Paris: Dunod.
7. Ghosh, S and Sharma, RP 2010. Pseudo-dynamic active response of non-vertical retaining walls upporting c–φ backfill. *Geotechnical and Geological Engineering* **28,** 633–641.
8. Kranz, E 1953. About anchored sheet piling. Communications from the field of hydraulic engineering and soil research <Über die Verankerung von Spundwänden. Mitteilungen aus dem Gebiet des Wasserbaues und der Baugrundforschung>. *Ernst & Sohn* **11**.
9. Mononobe, N and Et matsuo, H 1929. *On the determination of earth pressure during earthquake* . Proceedings of World Engineering congress, 177-185.
10. Richards, R, Huang, C and Fishman, K 1999. Seismic earth pressure on retaining structures. *Journal of Geotechnical and Geoenvironmental Engineering* **125**, 771-778.

11. Sahoo, PP, Shukla, SK and Mohyeddin, A 2018. Analytical expressions for determining the stability of cohesionless soil slope under generalized seismic conditions. *Journal of Mountain Science* **15,** 1559–1571.
12. Saran, S and Prakash, S 1968. Dimensionless parameters for static and dynamic earth pressures behind retaining walls. *Indian Geotechnical J*ournal **7**, 295 – 310.
13. Shukla, SK, Gupta, SK and Sivakugan, N 2009. Active earth pressure on retaining wall for c–φ soil backfill under seismic loading condition. *Journal of Geotechnical and Geoenvironmental Engineering* **135**, 690–696.
14. Whitlow, RB 1995. *Asic soil mechanics*. England: Wesley Longman.

Editor received the manuscript: 08.07.2020